MARCEL DEKKER, INC. • 270 MADISON AVENUE • NEW YORK, NY 10016

ANALYTICAL LETTERS
Vol. 36, No. 11, pp. 2427–2442, 2003

SENSORS AND BIOSENSORS

Disposable Nitrite Sensor Based on Hemoglobin-Colloidal Gold Nanoparticle Modified Screen-Printed Electrode

Xiaoxing Xu,[1,2] Songqin Liu,[1] Bing Li,[1] and Huangxian Ju[1,*]

[1]Department of Chemistry, State Key Laboratory of Coordination Chemistry, Institute of Chemical Biology, Nanjing University, Nanjing, China
[2]Department of Chemistry, Changshu College of Jiangsu, Changshu, China

ABSTRACT

An unmediated, disposable nitrite amperometric biosensor based on hemoglobin (Hb)-colloidal gold nanoparticle modified screen-printed carbon electrode (Hb-Au-SPCE) was proposed. The immobilized Hb showed a couple of quasi-reversible redox peak with a formal potential of −0.224 V (vs. SCE) in 0.2 mol dm^{-3} pH 5.5 NaAc-HAc buffer. The formal potential changed linearly between pH 4.0 to 9.0

*Correspondence: Huangxian Ju, Department of Chemistry, State Key Laboratory of Coordination Chemistry, Institute of Analytical Science, Nanjing University, Nanjing 210093, P.R. China; Fax: +86-25-3593593; E-mail: hxju@nju.edu.cn.

DOI: 10.1081/AL-120024333 0003-2719 (Print); 1532-236X (Online)

MARCEL DEKKER, INC. • 270 MADISON AVENUE • NEW YORK, NY 10016

with a slope of $-46.4\,\text{mV}\ \text{pH}^{-1}$. The Hb-Au-SPCE displayed a rapid amperometric response to the reduction of nitrite, which allowed to be used for the determination of nitrite with a linear range from 3.0×10^{-7} to $7.0 \times 10^{-4}\,\text{mol}\,\text{dm}^{-3}$ and a detection limit of $1.0 \times 10^{-7}\,\text{mol}\,\text{dm}^{-3}$ at 3σ. The amperometric sensor had a high sensitivity, good accuracy, and stability and is simple to use, lost-cost, rapid for the nitrite quantitative detection in practical applications.

Key Words: Screen-printed electrode; Biosensors; Nitrite; Hemoglobin; Colloidal gold; Amperometry; Electron transfer; Electrocatalysis.

INTRODUCTION

Nitrite is an important contamination in water, food products, and environmental matrices.[1,2] Ingested nitrite can react with amines and amides to form potent carcinogens, nitrosamines.[3] Therefore, reliable analytical procedures are required for its sensitivity determination in various matrices. Many techniques such as spectrophotometry,[4] chromatography,[5] capillary electrophoresis,[6] ion-exchange chromatography,[7] fluorimetry,[8] chemiluminescence,[9] and electrochemistry[10–16] have been commonly used for its monitoring. The electrochemical sensors based on iron porphyrin,[11] ruthenium polymer,[12] nitrite reductase,[13,14] and noble-metal-substituted polyoxometalates[15] have been developed for the determination of nitrite in egg, saliva, waste water, and pickled vegetable water. Most of these sensors have relatively good selectivity and fast response. However, it is difficult to get them sufficiently stable for exposing them directly to real samples due to fouling of the electrode surface,[16] denaturation of enzymes, or slow removal of modifiers from the surface. Another problem is the commercial unavailability of some modifiers, which limits their extensive application. In 1995, Neuhold et al.[17] prepared a carbon screen-printed electrode for the detection of nitrite in ground water and drinking water by mixing Aliquat 336 anion exchanger into a carbon ink prior to printing. This approach overcame previously time-consuming and could detect nitrite down to $30\,\mu\text{g}\,\text{dm}^{-3}$ ($0.65\,\mu\text{mol}\,\text{dm}^{-3}$) in standard solutions and $100\,\mu\text{g}\,\text{dm}^{-3}$ ($2.17\,\mu\text{mol}\,\text{dm}^{-3}$) in water samples. In this work we develop a novel nitrite sensor based on the immobilization of hemoglobin (Hb) on colloidal gold nanoparticle modified carbon screen-printed electrode. This sensor solves the problem mentioned above by combining the

advantageous features of colloidal gold nanoparticles and carbon screen-printed technology. It can detect nitrite down to $0.1\,\mu mol\,dm^{-3}$ and shows good accuracy and stability.

Recently, the application of screen-printed electrodes (SPCEs) has attracted an increasing interest due to their prominent characteristics, such as simple and inexpensive fabrication, convenience utility, and low cost.[18–20] Early screen-printed biosensors focused on the determination of glucose in blood samples.[21–23] Later the screen-printed biosensors broadened its applications to detect other biomolecules such as pesticides,[18] metals,[24] anions,[17,25] and potential pollutants.[26] Several mediators such as cobalt phthalocyanine,[23] hexacyanoferrate,[27] ferrocene derivative,[28] conducting polymer polypyrrole[29] and Prussian Blue microparticles,[20,30] and proteins or enzymes[31,32] have been incorporated into the carbon ink for sensor preparations. Here, colloidal gold nanoparticles are incorporated into the carbon ink to immobilize hemoglobin for preparation of a novel unmediated, disposable nitrite amperometric screen-printed biosensor. The direct electron transfer of immobilized hemoglobin is studied for the first time on a screen-printed electrode.

The direct electron transfer between Hb and electrodes has been achieved by incorporating Hb in polyacrylamide hydrogel,[32] surfactant,[33] clay[34] and SP Sephadex,[35] and DNA[36,37] modified membranes. Colloidal gold is an extensively used metal colloid, which has been used for study of direct electrochemistry of proteins such as HRP,[38] cytochrome c,[39,40] and hemoglobin.[41] It provides an environment similar to that of redox proteins in native systems and gives the protein molecules more freedom in orientation, thus reducing the insulating property of the protein shell for the direct electron transfer and facilitating the electron transfer through the conducting tunnels of colloidal gold.[42] This work reports a 2.0 fold increase in the cathodic peak current of immobilized hemoglobin in presence of colloidal gold nanoparticles and a good electrochemical response to the reduction of NO_2^- in presence of hemoglobin, producing a novel biosensor for nitrite.

EXPERIMENTAL

Material and Reagents

Bovine hemoglobin was purchased from Sigma (molecular weight 54,600) and used without further purification. Hb solution ($5.0\,mg\,mL^{-1}$) was prepared and stored at 4°C as stock solution. $K_3[Fe(CN)_6]$,

$HAuCl_4 \cdot 3H_2O$, and trisodium citrate dihydrate were purchased from Aldrich (Deisenhofen, Germany). Polyvinylchloride (PVC) was provided by Shanghai Chemical Reagent Co. Carbon graphite powder (<325 mesh, Johnson Matthey) and cellulose diacetate (from Shanghai Chemical Reagent Co) were used for preparation of carbon ink. Cellulose diacetate stock solution was prepared by dissolving 1.0 g cellulose diacetate in 100 mL 1:1 hexamethylene–acetone. All other chemicals were of analytical reagent grade and all solutions were prepared with deionized water of 18 MΩ purified from a Milli-Q purification system. Colloidal gold nanoparticles with diameter of 24 ± 2 nm were prepared and stored according to literature.[40,41] Unless specifically indicated, the buffer used in this work was 0.2 mol dm^{-3} pH 5.5 NaAc-HAc. Zero point one mole per cubic decimeter phosphate buffer solutions (PBS) with various pH values used to investigate the dependence of the direct electrochemistry of immobilized hemoglobin on pH were prepared by mixing stock standard solutions of K_2HPO_4 and KH_2PO_4 and adjusting the pH with 0.1 mol dm^{-3} H_3PO_4 or NaOH.

Sensor Preparation

The screen-printed carbon ink electrode was prepared by using a screen-printed technology as follows. Silver ink was firstly printed onto PVC substrate to form conducing track (30×1 mm^2). This surface was washed thoroughly with NaOH solution and then deionized water. A mixture of 10 mg of pretreated graphite powder with 20 μL colloidal gold solution was prepared. Following evaporation of water in the air, 30 μL cellulose diacetate solution was added to the mixture to obtain colloidal gold nanoparticle modified screen-printed carbon ink (Au-SPC). As a comparison, 10 mg of graphite powder was mixed thoroughly with 30 μL cellulose diacetate solution without the presence of colloidal gold nanoparticles to obtain screen-printed carbon ink (SPC). The resulting inks were then printed onto above silver conducting tracks to form colloidal gold nanoparticle modified screen-printed carbon electrode (Au-SPCE) and screen-printed carbon electrode (SPCE). The electrodes were insulated by overlaying a silicone rubber layer to expose only the conductive terminal and the working surface with an area of ca. 10 mm^2. The immobilization of hemoglobin was carried out by dropping 10 μL of Hb solution onto the working surface of the SPCE or Au-SPCE and dried overnight under room temperature to obtain Hb-SPCE or Hb-Au-SPCE. The modified electrodes were rinsed with ethanol and water and stored at 4°C when not in use.

Electrochemical Measurements

Electrochemical experiments were carried out with a BAS-100A electrochemical analyzer at room temperature ($18 \pm 2^{\circ}C$). A three-electrode cell was equipped with a saturated calomel electrode (SCE), a platinum wire and a SPCE, Hb-SPCE, Au-SPCE, or Hb-Au-SPCE as reference, counter, and working electrode, respectively. The real geometry area of the working electrode was determined to be $0.11\,cm^2$ by the slope of plot of the anodic peak current of $2.5\,mmol\,dm^{-3}$ $K_3[Fe(CN)_6]$ in $0.1\,mol\,dm^{-3}$ KCl vs. the square root of scan rate. All experimental solutions were deoxygenated by bubbling highly pure nitrogen for 20 min and maintained under nitrogen atmosphere during the course of the experiment.

RESULTS AND DISCUSSION

Electrochemical Characterization of the Screen-Printed Electrodes

The screen-printed carbon electrodes were characterized by means of charging current measurements and cyclic voltammograms of $K_3[Fe(CN)_6]$ solution. The charging currents were determined from the cyclic voltammograms of these electrodes at $50\,mV\,s^{-1}$. The screen-printed carbon electrodes showed the charging current of $22\,\mu A$ at 0.0 V and $16\,\mu A$ at 0.4 V (as shown in Fig. 1a). After the screen-printed carbon electrode was modified with colloidal gold nanoparticles, the charging current decreased to $8.3\,\mu A$ at 0.0 V and $6.3\,\mu A$ at 0.4 V (Fig. 1b). The Au-SPCE displayed a couple of stable and well-defined redox peaks of $K_3[Fe(CN)_6]$ at 241 and 172 mV with the peak currents of 32.3 and $28.5\,\mu A$, respectively. Although the SPCE also exhibited a couple of redox peaks of $K_3[Fe(CN)_6]$ with the peak currents of 23.1 and $20.0\,\mu A$, the peak-to-peak separation of 134 mV was much larger than that of 69 mV at Au-SPCE, which was close to theoretical value of the reversible one electron electrode reaction.

Figure 2 shows the cyclic voltammograms of $K_3[Fe(CN)_6]$ at Au-SPCE at different scan rates. The redox peak currents were proportional to the square root of the scan rate (Fig. 2A). The plot of anodic peak potential vs. the logarithm of scan rate gave a slope of 0.0249 (Fig. 2B), thus the charge transfer coefficient, α, was 0.51 ($n = 1$). From the peak-to-peak separations at the scan rate range from 20 to $200\,mV\,s^{-1}$, the Nicholson's equation[43] and its diffusion coefficient

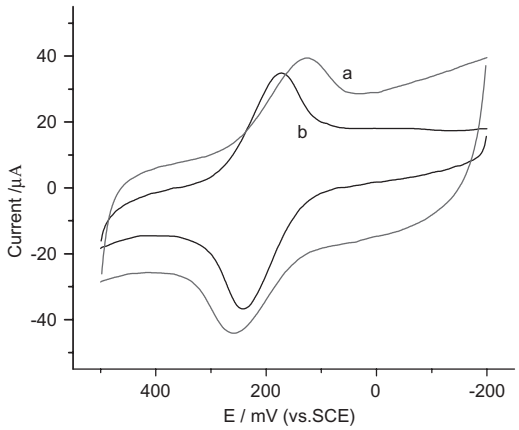

Figure 1. Cyclic voltammograms of SPCE (a) and Au-SPCE (b) in $0.25\,\text{mmol}\,\text{dm}^{-3}$ $K_3Fe(CN)_6 + 0.1\,\text{mol}\,\text{dm}^{-3}$ KCl solution at $50\,\text{mV}\,\text{s}^{-1}$.

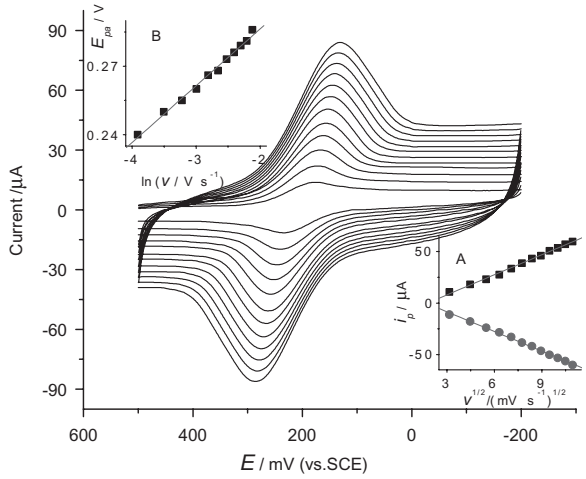

Figure 2. Cyclic voltammograms of Au-SPCE in $0.25\,\text{mmol}\,\text{dm}^{-3}$ $K_3Fe(CN)_6 + 0.1\,\text{mol}\,\text{dm}^{-3}$ KCl solution at 10, 20, 30, 40, 50, 60, 70, 80, 90, 100, 110, and $120\,\text{mV}\,\text{s}^{-1}$. Inset: plots of peak currents vs. $\nu^{1/2}$ (A) and plot of anodic peak potential vs. ln(ν) (B).

of 7.6×10^{-6} $\text{cm}^2\,\text{s}^{-1}$,[44] the average electron transfer rate constant, k^0, for heterogeneous electron transfer was calculated to be $(6.8 \pm 0.7) \times 10^{-3}\,\text{cm}\,\text{s}^{-1}$. The k^0 value of $K_3[Fe(CN)_6]$ at Au-SPCE was about 4.6 times that of $1.48 \times 10^{-3}\,\text{cm}\,\text{s}^{-1}$ at carbon paste electrode

obtained by RDE in the same supporting electrolyte.[45] Thus, the presence of colloidal gold nanoparticles not only improved the conductivity of SPCE and amplified the electrochemical signals, but also increased the electron transfer rate.

Direct Electrochemistry of Hemoglobin Immobilized at Au-SPCE

When SPCE and Au-SPCE were cyclically scanned in buffer solution containing of 0.1 mmol dm^{-3} Hb, no obvious peak was observed, thus the electron transfer between these electrodes and Hb in solution was very slow or not at all. However, Hb-Au-SPCE gave a couple of stable and well-defined redox peaks at $-(177 \pm 2)$ mV and $-(270 \pm 2)$ mV at 50 mV s^{-1} in NaAc-HAc buffer (curve d in Fig. 3). No peak was observed at both SPCE and Au-SPCE (curves a and b in Fig. 3). Au-SPCE displayed lower background current than SPCE. Obviously, the response of Hb-Au-SPCE was attributed to the redox of the electroactive center of the immobilized Hb. Without presence of gold colloid nanoparticles, Hb-SPCE also showed the response of Hb. The cathodic response, however, was 2.0 fold smaller than that of Hb-Au-SPCE (Fig. 3c). Thus, the colloidal gold nanoparticles played an important role in improving the electrochemical response and facilitating the electron exchange between the Hb and carbon particles. The formal potential of the heme Fe(III/II)

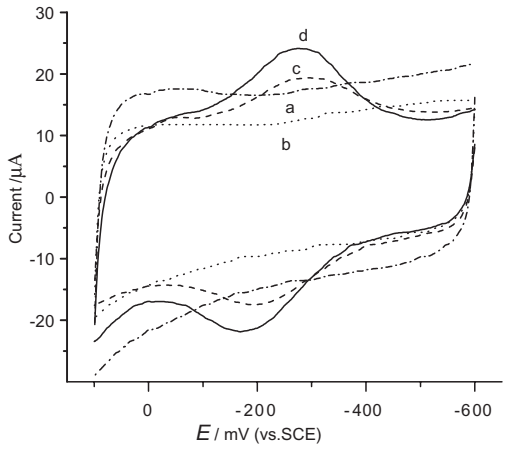

Figure 3. Cyclic voltammograms of SPCE (a), Au-SPCE (b), Hb-SPCE (c), and Hb-Au-SPCE (d) in 0.2 M pH 5.5 NaAc-HAc buffer at 50 mV s^{-1}.

couple of Hb in Hb-Au-SPCE at pH 5.5, estimated as the midpoint of the anodic and cathodic peak potentials, was −224 mV (vs. SCE). This value was similar to native hemoglobin in solution (−0.22 V),[46] suggesting that most Hb molecules preserved their native structure after the adsorption process.

With an increasing scan rate the redox peak currents of the immobilized Hb increased and its anodic peak potential shifted to a more positive value, while the cathodic peak potential shifted in a negative direction. The anodic and cathodic peak currents (i_{pa} and i_{pc}) were proportional to the scan rate, thus the electrode reaction was typical of surface-controlled quasi-reversible process. The slope of the plot of anodic peak potential vs. the logarithm of scan rate gave a charge transfer coefficient of 0.52 ($n = 1$). Considering the peak-to-peak separations less than 200 mV, the electron transfer rate k_s could be estimated with the formula[47] $k_s = mnFv/RT$, where m is a parameter related to the peak-to-peak separation. The peak-to-peak separations were 81, 92, 107, 122, 133, 141, 153, 165, 178, 188, and 197 mV at 50, 75, 100, 125, 150, 175, 200, 225, 250, 275, and 300 mV s^{-1}, respectively, producing an average k_s value of $(0.91 \pm 0.09)\ s^{-1}$.

Influence of Solution pH on Electrochemical Behaviors of Immobilized Hemoglobin

Figure 4 shows the effect of solution pH on the electrochemical behaviors of Hb immobilized on Au-SPCE. With an increasing solution pH from 4.0 to 9.0 both reduction and oxidation peak potentials shifted negatively. Moreover, all changes in the peak potentials and currents with solution pH were reversible. The plots of the peak potentials vs. pH gave two lines with the same slope of −46.4 mV pH^{-1} (inset A in Fig. 4), which was close to the expected value of −57.8 mV pH^{-1} for the one proton and one electron participating electron transfer process at 291.2 K.[33,35]

Inset B in Fig. 4 shows the relationship between the peak currents of the immobilized Hb and solution pH. It was clearly observed that an optimal pH range occurred between 4.0 and 7.0 with the maximum values at pH 5.5.

Amperometric Response of Nitrite at Hb-Au-SPCE

Figure 5 shows the cyclic voltammograms of Au-SPCE and Hb-Au-SPCE in pH 5.5 NaAc-HAc buffer containing different concentrations of

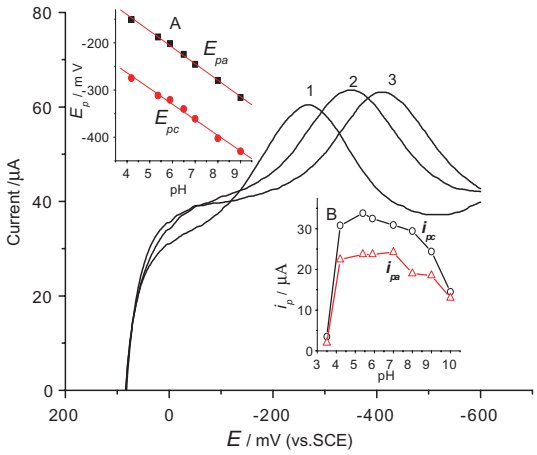

Figure 4. The cathodic segments of cyclic voltammograms of Hb-Au-SPCE in 0.1 mol dm^{-3} PBS at pH 5.0 (1), 7.0 (2), and 9.0 (3) at 100 mV s^{-1}. Inset: plots of peak potential (A) and peak current (B) vs. pH.

nitrite. At Hb-Au-SPCE a new irreversible reduction peak occurred at −780 mV at 100 mV s^{-1} upon addition of $NaNO_2$ to the buffer (Fig. 5A). However, only very small current change was observed at Au-SPCE in the same conditions (Fig. 5B). Thus, nitrite was not efficiently reduced in the studied potential range at Au-SPCE. The presence of immobilized Hb promoted the reduction of nitrite at the colloidal gold nanoparticle modified screen-printed carbon electrode. Furthermore, with the increasing nitrite concentration the reduction peak current at Hb-Au-SPCE increased.

Figure 6 shows a typical hydrodynamic current-time response of the Hb-Au-SPCE at −800 mV upon successive additions of $NaNO_2$ to 0.2 mol dm^{-3} pH 5.5 NaAc-HAc buffer. Upon the addition, the sensor achieved 95% of its steady-state current within 10 s, indicating a fast amperometric response to nitrite reduction. The calibration curve of the sensor to nitrite concentration was shown in inset in Fig. 6. The linear response range of the sensor to nitrite concentration was from 3.0×10^{-7} to 7.0×10^{-4} mol dm^{-3} with a correlation coefficient of 0.9991. From the slope of 0.032 μA μM^{-1} the detection limit was estimated to be 1.0×10^{-7} mmol dm^{-3} at 3σ. The sensitivity was much better than the limit of 5.0×10^{-4} mol dm^{-3} reported previously.[48] The sensor based on the Hb-Au-SPCE displayed a higher sensitivity for nitrite determination.

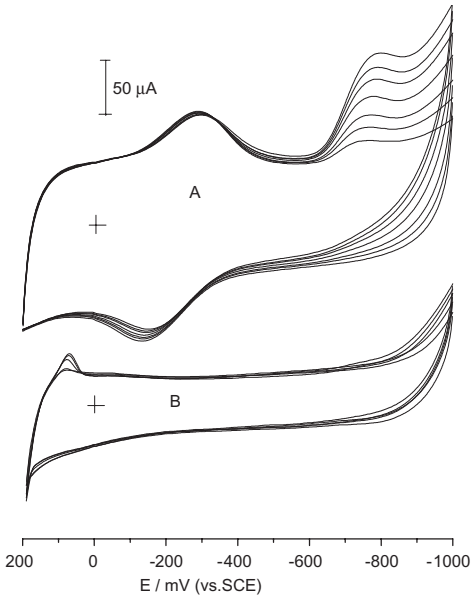

Figure 5. Cyclic voltammograms of Hb-Au-SPCE (A) and Au-SPCE (B) in 0.2 M pH 5.5 NaAc-HAc buffer containing 0.2, 0.4, 0.6, 1.0, 1.5, 2.0, and 2.5 mmol dm^{-3} $NaNO_2$ (from inner to outer) at 100 mV s^{-1}.

Analytical Application

The common ions were tested to examine the possible interference with the detection of nitrite. The criterion of the interference was based on the current response. If the addition of given ion caused a current charge of 10% or more, it was considered to interfere with the determination of nitrite. The detection results indicated that Na^+, K^+, and Cl^- did not interfere with nitrite determination, Ca^{2+}, Mg^{2+}, Al^{3+}, Mn^{2+}, Cu^{2+}, Zn^{2+}, SO_4^{2-}, and CO_3^{2-} at the concentrations 20 times $NaNO_2$ of 0.5 mmol dm^{-3} did not show any interference. Thus, this sensor exhibited a good selectivity.

The synthetic samples were prepared by adding the standard solution of nitrite into a tap water to obtain the final concentrations of 5.0, 10, and 20 μmol dm^{-3}. The results of three determinations for each sample using the sensor showed the recoveries from 95 to 104% and relative standard deviations less than 3.5%. Both the recovery and precision were satisfactory. Thus, this sensor could be used for nitrite determination in practical samples.

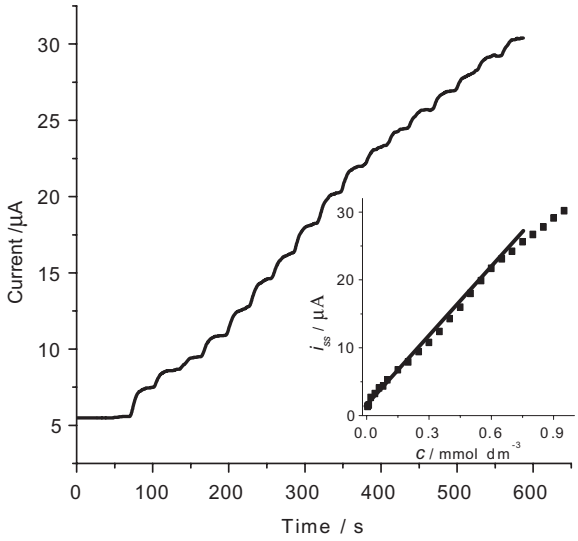

Figure 6. Typical steady-state response of the sensor with an increasing $NaNO_2$ concentration by 5.0 μmol dm^{-3} each step at −0.8 V. Inset: the linear correlation curve.

Stability of the Sensor

When the sensor was stored at 4°C for two weeks, no obvious decrease in the response to NO_2^- was observed. After a storage period of four weeks, the sensor retained 90% of its initial current response. The sensor retained 80% of its initial current response after a storage period of three months. Thus, the stability of the sensor was very good. It could also be stored in air without any special protection step, and showed a stable response during at least 10 days. At the same time the electrode could be carried out more than 100 measurements without noticeable signal decrease.

CONCLUSIONS

This work proposes a novel disposable biosensor for nitrite based on the immobilization of hemoglobin on the colloidal gold nanoparticle modified screen-printed carbon electrode. The colloidal gold nanoparticles not only decrease the background current, improve the conductivity,

and amplify the electrochemical signals of screen-printed carbon electrode, but also retain the bioactivity of immobilized protein and accelerate the electron transfer rate. The sensor shows a highly sensitive response to nitrite, satisfactory recovery and precision, good selectivity and stability, and can be used for determination of nitrite with a wide concentration range in a real sample.

ACKNOWLEDGMENTS

This project was supported by the National Natural Science Foundation of China (No. 20275017, 90206037), the Specialized Research Funds for the Excellent Young Teachers from Chinese Ministry of Education, the Science Foundation of Jiangsu (No. BS2001063) and the Key Project of Cancer Institute of Jiangsu Province.

REFERENCES

1. Fox, J.B. The determination of nitrite: a critical review. Crit. CRC Rev. Anal. Chem. **1985**, *15*, 283–313.
2. Dumham, A.J.; Barkley, R.M.; Sievers, R.E. Aqueous nitrite ion determination by selective reduction and gas phase nitric oxide chemiluminescence. Anal. Chem. **1995**, *67*, 220–224.
3. Lijinsky, W.; Epstein, S.S. Nitrosamines as environmental cancinogens. Nature **1970**, *225*, 21–23.
4. American Public Health Association. *Standard Methods for the Examination of Water and Waste Water*; New York, 1995.
5. Jain, A.; Smith, R.M.; Verma, K.K. Gas chromatographic determination of nitrite in water by precolumn formation of 2-phenylphenol with flame ionization detection. J. Chromatogr. A **1997**, *760*, 319–325.
6. Trushina, E.V.; Oda, R.R.; Landers, J.P.; McMurray, C.T. Determination for nitrate and nitrite reduction by capillary ion electrophoresis. Electrophoresis **1997**, *18*, 1890–1898.
7. Preik-Steinhoff, H.; Kelm, M. Determination of nitrite in human blood by combination of a specific sample preparation with high-performance anion-exchange chromatography and electrochemical detection. J. Chromatogr. B **1996**, *685*, 348–352.

8. Jie, N.; Si, Z.; Yang, J.; Miao, Z.; Huang, X.; Zhang, Q.; Song, Z. Fluorometric determination of traces of nitrite with rhodamine 6G. Microchem. J. **1997**, *55*, 351–356.
9. Yang, F.; Troncy, M.; Francoeur, E.; Vinet, B.; Vinay, P.; Czaika, G.; Blaise, G. Effects of reducing reagents and temperature on conversion of nitrite and nitrate nitric oxide and detection of NO by chemiluminescence. Clin. Chem. **1997**, *43*, 657–662.
10. Cox, J.A.; Kulesza, P.J. A selective electrolytic sensor for nitrite based on a modified platinum electrode. Anal. Chim. Acta **1984**, *158*, 335–341.
11. Barley, M.H.; Takeuchi, K.J.; Meyer, T.J. Electrocatalytic reduction of nitrite to ammonia based on a water-soluble iron porphyrin. J. Am. Chem. Soc. **1986**, *108*, 5876–5885.
12. O'Shea, T.J.; Leech, D.; Smyth, M.R.; Vos, J.G. Determination of nitrite based on mediated oxidation at a carbon paste electrode modified with a ruthenium polymer. Talanta **1992**, *39*, 443–447.
13. Mellor, R.B.; Ronnenberg, J.; Campbell, W.H.; Diekmann, S. Reduction of nitrate and nitrite in water by immobilized enzymes. Nature **1992**, *355*, 717–719.
14. Strehlitz, B.; Grundig, B.; Schumacher, W.; Kroneck, P.M.H.; Vorlop, K.D.; Kotte, H. A nitrite sensor based on a highly sensitive nitrite reductase mediator-coupled amperometric detection. Anal. Chem. **1996**, *68*, 807–816.
15. Sun, W.; Zhang, S.; Lin, X.; Jin, L.; Jin, S.; Deng, J.; Kong, J. Electrocatalytic reduction of nitrite at a carbon fiber microelectrode chemically modified by palladium(II)-substituted Dawson type heptadecatungstodiphosphate. J. Electroanal. Chem. **1999**, *469*, 63–71.
16. Larsen, L.H.; Damgaard, L.R.; Kjaer, T.; Stenstrom, T.; Lynggard-Jensen, A.; Revsbech, P. Fast responding biosensor for on-line determination of nitrate/nitrite in activated sludge. Wat. Res. **2000**, *34*, 2463–2468.
17. Neuhold, G.G.; Wang, J.; Cai, X.; Kalcher, K. Screen-printed electrodes for nitrite based on anion-exchanger-doped carbon inks. Analyst **1995**, *120*, 2377–2380.
18. Palchetti, I.; Cagnini, A.; Del Carlo, M.; Coppi, C.; Mascini, M.; Tuiner, A.P.F. Determination of anticholinesterase pesticides in real samples using s disposable biosensor. Anal. Chim. Acta **1997**, *337*, 315–321.
19. Hart, J.P.; Wring, S.A. Recent developments in the design and application of screen-printed electrochemical sensors for

biomedical, environmental and industrial analyses. Trends Anal. Chem. **1997**, *16*, 89–103.
20. O'Halloran, M.P.; Pravda, M.; Guilbault, G.G. Prussian Blue bulk modified screen-printed electrodes for H_2O_2 detection and for biosensors. Talanta **2001**, *55*, 605–611.
21. Cass, A.E.G.; Davis, G.; Francis, G.D.; Hill, H.A.O.; Aston, W.J.; Higgins, I.J.; Plotkin, E.V.; Scott, L.D.L.; Turner, A.P.F. Ferrocene-mediator enzyme electrode for amperometric determination of glucose. Anal. Chem. **1984**, *56*, 667–671.
22. Morris, N.A.; Cardosi, M.F.; Birch, B.J.; Turner, A.P.F. An electrochemical capillary fill device for the analysis of glucose incorporating glucose oxidase and ruthenium(III) hexamine as mediator. Electroanalsis **1992**, *4*, 1–9.
23. Gilmartin, M.A.T.; Hart, J.P.; Patton, D.T. Prototype, solid-phase, glucose biosensor. Analyst **1995**, *120*, 1973–1981.
24. Wang, J.; Tian, B. Screen-printed stripping voltammetric/potentiometric electrodes for decentralized testing of trace lead. Anal. Chem. **1992**, *64*, 1706–1709.
25. Fogg, A.G.; Scullion, S.P.; Edmonds, T.E.; Birch, B.J. Adaptation of on-line reactions developed for use with flow injection with amperometric detection for use in disposable sensor devices: reductive determination of phosphate as pre-formed 12-molybdophosphate in a capillary-fill device. Analyst **1990**, *115*, 1277–1281.
26. Wang, J.; Pamidi, P.V.A. Disposable screen-printed electrodes for monitoring hydrazines. Talanta **1995**, *42*, 463–467.
27. Marcinkeviciene, J.; Kulys, J. Berlin's network of natural waters and its nutrient pollution (Germany). Biosens. Bioelectron. **1993**, *8*, 209–212.
28. Nagata, R.; Yokayama, K.; Clark, S.A.; Karube, I. A glucose sensor fabricated by the serene printing technique. Biosens. Bioelectron. **1995**, *10*, 261–267.
29. Koopal, C.G.J.; Bos, A.A.; Nolte, R.J.M. Third-generation glucose biosensor incorporated in a conducting printing ink. Sens. Actuators B **1994**, *18–19*, 166–170.
30. Ricci, F.; Amine, A.; Palleschi, G.; Moscone, D. Prussian Blue based screen printed biosensors with improved characteristics of long-term lifetime and pH stability. Biosens. Bioelectron. **2003**, *18*, 165–174.
31. Abass, A.K.; Hart, J.P.; Cowell, D. Development of an amperometric sulfite biosensor based on sulfite oxidase with cytochrome c, as electron acceptor, and a screen-printed transducer. Sens. Actuators B **2000**, *62*, 148–153.

32. Abass, A.K.; Hart, J.P. Direct electrochemistry of cytochrome c at plain and membrane modified screen-printed carbon electrodes. Electrochim. Acta **2001**, *46*, 829–836.
33. Sun, H.; Hu, N.; Ma, H. Direct electron transfer at horseradish peroxidase-colloidal gold modified electrodes. Electroanalysis **2000**, *12*, 1064–1070.
34. Rusling, J.F. Enzyme bioelectrochemistry in cast biomembrane-like films. Acc. Chem. Res. **1998**, *31*, 363–369.
35. Chen, X.; Hu, N.; Zeng, Y.; Rusling, J.F.; Yang, J. Ordered electrochemically active films of hemoglobin, didodecyldimethylammonium ions and clay. Langmuir **1999**, *15*, 7022–7030.
36. Fan, C.; Wang, H.; Sun, S.; Zhu, D.; Wagner, G.; Li, G. Electron-transfer reactivity and enzymatic activity of hemoglobin in a SP sephadex membrane. Anal. Chem. **2001**, *73*, 2850–2854.
37. Fan, C.; Li, G.; Zhu, J.; Zhu, D. A reagentless nitric oxide biosensor based on hemoglobin–DNA films. Anal. Chim. Acta **2000**, *423*, 95–100.
38. Zhao, J.; Stonchuerner, R.W.; O'Daly, J.P.; Crumbliss, A.L. Direct electron transfer at horseradish peroxidase-colloidal gold modified electrodes. J. Electroanal. Chem. **1992**, *327*, 109–119.
39. Brown, K.R.; Fox, A.P.; Natan, M.J. Electrochemistry of cytochrome c at Au colloid-modified SnO_2 electrodes. J. Am. Chem. Soc. **1996**, *118*, 1154–1157.
40. Ju, H.X.; Liu, S.Q.; Ge, B.; Lisdat, F.; Scheller, F.W. Electrochemistry of cytochrome c immobilized on colloidal gold modified carbon paste electrodes and its electrocatalytic activity. Electroanalysis **2002**, *14*, 141–147.
41. Gu, H.Y.; Yu, A.M.; Chen, H.Y. Direct electron transfer and characterization of hemoglobin immobilized on a Au colloid cysteamine-modified gold electrode. J. Electroanal. Chem. **2001**, *516*, 119–126.
42. Liu, S.Q.; Leech, D.; Ju, H.X. Application of colloidal gold in protein immobilization, electron transfer and biosensing. Anal. Lett. **2003**, *36*, 1–19.
43. Nicholson, R.S. Theory and application of cyclic voltammetry for measurement of electrode reaction kinetics. Anal. Chem. **1965**, *38*, 1351–1355.
44. Stackelberg, I.M.V.; Pilgram, M.; Toome, V. Determination of diffusion coefficients of several ions in aqueous solutions in the presence of foreign electrolytes. Z. Elektro. Chem. **1953**, *57*, 342–350.
45. Galus, Z.; Adams, R.N. Low-temp voltammetry and electron paramagnetic resonance studies. J. Phys. Chem. **1963**, *67*, 866–891.

46. Lu, Z.; Dong, S. Rapid redox reaction of hemoglobin at methylene green modified platinum electrode. Electrochim. Acta **1990**, *35*, 1139–1143.
47. Laviron, E. General expression of the linear potential sweep voltammogram in the case of diffusionless electrochemical systems. J. Electroanal. Chem. **1979**, *101*, 19–28.
48. McCormac, T.; Fabre, B.; Bidan, G.J. Part II. Role of pH and the transition metal for the electrocatalytic reduction of nitrite with transition metal substituted Dawson type heteropolyanions. J. Electroanal. Chem. **1997**, *427*, 155–159.

Received April 26, 2003
Accepted May 20, 2003